

Exploring the Arabidopsis sulfur metabolome

Katharina Gläser¹, Basem Kanawati², Tobias Kubo³, Philippe Schmitt-Kopplin² and Erwin Grill^{1,*}

¹Lehrstuhl für Botanik, Technische Universität München, Emil-Ramann Straße 4, D-85354, Freising, Germany,

²Analytical Biogeochemistry, Helmholtz Zentrum München – Deutsches Forschungszentrum für Gesundheit und Umwelt, D-85764, Neuherberg, Germany, and

³Anorganisch-Chemisches Institut, Technische Universität München, Poststelle, Alte Akademie 1, 85354 Freising, Germany

Received 19 July 2013; revised 9 October 2013; accepted 16 October 2013.

*For correspondence (e-mail erwin.grill@wzw.tum.de).

SUMMARY

Sulfur plays a crucial role in protein structure and function, redox status and plant biotic stress responses. However, our understanding of sulfur metabolism is limited to identified pathways. In this study, we used a high-resolution Fourier transform mass spectrometric approach in combination with stable isotope labeling to describe the sulfur metabolome of *Arabidopsis thaliana*. Databases contain roughly 300 sulfur compounds assigned to *Arabidopsis*. In comparative analyses, we showed that the overlap of the expected sulfur metabolome and the mass spectrometric data was surprisingly low, and we were able to assign only 37 of the 300 predicted compounds. By contrast, we identified approximately 140 sulfur metabolites that have not been assigned to the databases to date. We used our method to characterize the γ -glutamyl transferase mutant *ggt4-1*, which is involved in the vacuolar breakdown of glutathione conjugates in detoxification reactions. Although xenobiotic substrates are well known, only a few endogenous substrates have been described. Among the specifically altered sulfur-containing masses in the *ggt4-1* mutant, we characterized one endogenous glutathione conjugate and a number of further candidates for endogenous substrates. The small percentage of predicted compounds and the high proportion of unassigned sulfur compounds identified in this study emphasize the need to re-evaluate our understanding of the sulfur metabolome.

Keywords: GGT4, γ -glutamyl transferase, glutathione conjugates, isotope labeling, ICR-FTMS, metabolomics, *Arabidopsis thaliana*.

INTRODUCTION

Sulfur is an essential mineral nutrient that plays a major role in the structure and function of proteins, co-enzymes, prosthetic groups and vitamins in all organisms (Kopriva *et al.*, 2009). In contrast to animals, plants are able to assimilate inorganic sulfate. Although the primary sulfur assimilation pathway in plants is well described, the nutrient-metabolic network is still poorly understood (Nikiforova *et al.*, 2004; Lee *et al.*, 2012; Omranian *et al.*, 2012). Sulfur deprivation, for example, has profound consequences on nitrogen nutrition and oxidative stress responses, which affect the growth, quality and yield of plants, particularly crops (Blake-Kalff *et al.*, 1998; Zhao *et al.*, 1999; Maruyama-Nakashita *et al.*, 2003; Hirai *et al.*, 2004; Nikiforova *et al.*, 2005). Accordingly, sulfur uptake and distribution underlie rigorous control mechanisms that are activated in response to developmentally or environmentally induced changes in nutrient demand (Yoshimoto *et al.*, 2003; Buchner *et al.*, 2004).

Assimilated sulfate is first activated to form adenosine-5'-phosphosulfate, which is reduced to sulfide for incorporation into cysteine (Cys). Alternatively, adenosine-5'-phosphosulfate may be further phosphorylated to form phospho-adenosine-5'-phosphosulfate for sulfation reactions in secondary metabolism (Mugford *et al.*, 2011; Ravilious and Jez, 2012). However, cysteine is the central intermediate for the synthesis of sulfur compounds in plants, while the major reservoir of non-protein reduced sulfur is the cysteine-containing tripeptide glutathione (GSH) (Hell and Wirtz, 2011). GSH plays a critical role in homeostasis and cellular defense, including redox status, signal transduction and detoxification (Noctor *et al.*, 2011). GSH forms conjugates with electrophilic compounds such as heavy metal ions or xenobiotics via its sulfhydryl group, either spontaneously or via the action of glutathione S-transferases (Edwards and Dixon, 2005; Cummins *et al.*, 2011). Higher plants contain a large number of glutathione

S-transferases, with more than 50 family members present in Arabidopsis, with functions assigned to xenobiotic detoxification and redox control.

Glutathione conjugates (GS conjugates) may be further processed by removal of either the glycine or the γ -glutamyl residue of the GSH moiety, with the latter reaction being catalyzed by γ -glutamyl transferases (GGTs) and glutamyl-peptidases (GGPs) (Grzam *et al.*, 2007; Geu-Flores *et al.*, 2009, 2011). Among the three functional GGT genes identified in Arabidopsis, GGT4 (At4 g29210) is specifically involved in vacuolar GS conjugate breakdown, while GGT1 and GGT2 are apoplastic and show a tissue-specific localization in leaves and developing siliques, respectively (Storozhenko *et al.*, 2002; Ohkama-Ohtsu *et al.*, 2007a,b). GS conjugates are also a substrate of phytochelatin synthase, which processes GS conjugates by its γ -glutamyl-cysteinyl (γ EC) transferase activity, generating γ EC conjugates in the cytosol, similar to cytosolic carboxypeptidases (Beck *et al.*, 2003; Blum *et al.*, 2007, 2010; Ohkama-Ohtsu *et al.*, 2008).

GS conjugates of xenobiotics, including the herbicides atrazin, alachlor and fluorodifen, are well documented (Öztetik, 2008). However, knowledge of GS conjugates of endogenous compounds is very limited. Some of these glutathionylated plant metabolites are highly unstable intermediates, such as isothiocyanates and oxilipins (Davoine *et al.*, 2006; Halkier and Gershenzon, 2006; Dixon *et al.*, 2010; Agerbirk and Olsen, 2012). Furthermore, it has been postulated that the sulfur in the thioglycoside bond of glucosinolates is derived from GSH. Mutant analysis supports conjugation of an aldoxime precursor to GSH, which is further processed by cytosolic GGP, a carboxypeptidase and a specific C-S-lyase, removing most of the GSH moiety and generating the sulfur conjugate as an intermediate of glucosinolate biosynthesis (Sønderby *et al.*, 2010; Geu-Flores *et al.*, 2011). For example, endogenous GS conjugates of indol-3-acetonitrile and fatty acid derivatives have been identified (Böttcher *et al.*, 2009; Dixon and Edwards, 2009).

The paucity of endogenous GS conjugates identified to date may be due to efficient turnover, resulting in low levels of these compounds in plants. Recent advances in metabolomic analysis have provided tools to overcome this bottleneck. Stable isotope labeling of proteins and metabolites in conjunction with sensitive, high-resolution mass spectrometry allow targeted identification and relative quantification of cellular compounds (Giavalisco *et al.*, 2008; Schütz *et al.*, 2011; Creek *et al.*, 2012). Recently, we used isotopic dimethylation to analyze the conjugation activity of Arabidopsis glutathione S-transferases in yeast (Krajewski *et al.*, 2013). In the current study, we performed *in vivo* labeling of the sulfur metabolome of Arabidopsis using the isotopes ^{32}S and ^{34}S in combination with ultra-high-resolution mass spectrometry.

When we analyzed crude extracts of Arabidopsis seedlings, we detected approximately 12 000 masses in the

negative ionization mode, of which 1.2% contain sulfur. Combination of positive and negative ionization led to approximately 200 unique sulfur compounds being identified. The analyses covered 37 annotated sulfur metabolites from plants, and allowed at least the determination of the elemental composition of the other sulfur metabolites in most cases. Comparative analysis of the Arabidopsis *ggt4-1* mutant revealed that deficiency in the vacuolar GGT results in accumulation of several sulfur-containing metabolites, including candidates for endogenous GS conjugates, and a concomitant decrease in respective Cys conjugates.

RESULTS

Sulfur isotope labeling in Arabidopsis

The cysteine autotrophy of plants allows labeling of sulfur-containing metabolites by feeding of stable sulfur isotope anions (Giavalisco *et al.*, 2011; Hsieh *et al.*, 2012). In order to determine the degree of isotope labeling and to optimize the strategy for labeling sulfur-containing compounds in Arabidopsis, seeds were germinated and seedlings were grown in the presence of various concentrations of ^{34}S -sulfate. Crude extracts were analyzed by direct-infusion ion cyclotron-resonance Fourier transformation mass spectrometry (DI-ICR-FTMS), which allows semi-quantitative analyses of metabolites (Walker *et al.*, 2011; Krajewski *et al.*, 2013). The applied extraction method allows the recovery of soluble, polar compounds with a preference for hydroxylated or carboxylated metabolites. Abundant sulfur-containing compounds of Arabidopsis are GSH, the S-adenosyl methionine catabolite S-ribosyl homocysteine (RHC) and neoglucobrassicin (1MOI3M), which is the most abundant glucosinolate in roots (Petersen *et al.*, 2002; Brown *et al.*, 2003; Hesse *et al.*, 2004). These compounds were identified by exact mass in the MS analysis, and served as reference substances for estimating the labeling efficiency (Figure 1).

Supplementing the nutrient solution with various concentrations of $^{34}\text{SO}_4^{2-}$ resulted in efficient incorporation of the heavy isotope in all three reference compounds within 2 weeks of cultivation (Figure 1a). Labeling efficiency was calculated by relating the mass signal of the heavy isotope to the sum of the corresponding ^{32}S and ^{34}S signals. Approximately saturating levels of ^{34}S labeling were observed upon supplementation with 0.75 mM $^{34}\text{SO}_4^{2-}$, with minor increases at 1.5 mM for RHC and GSH. The heavy sulfur isotope of 1MOI3M reached levels of 95%, while the labeling efficiencies of GSH and RHC were 83 and 74%, respectively. By using a half-saturating $^{34}\text{SO}_4^{2-}$ concentration, a characteristic 'double' peak pattern is obtained by the presence of both ^{32}S and ^{34}S isotopic signals in the spectra for the ^{34}S -labeled samples with approximately equal intensities. In a kinetic analysis performed using 0.36 mM sulfate,

Figure 1. Efficiency of ^{34}S isotope labeling of *Arabidopsis* seedlings.

Efficiency is expressed as the percentage of ^{34}S incorporation into glutathione (GSH), *S*-ribosyl homocysteine (RHC) or neoglucobrassicin (1MOI3M).

(a) Influence of $^{34}\text{SO}_4^{2-}$ concentrations on the labeling of sulfur compounds. Seedlings were grown for 2 weeks on sulfur-free medium supplemented with various concentrations of $\text{Na}_2^{34}\text{SO}_4$.

(b) Dependence of sulfur labeling efficiency on the exposure time. Seedlings were cultivated in the presence of 0.36 mM $\text{Na}_2^{34}\text{SO}_4$.

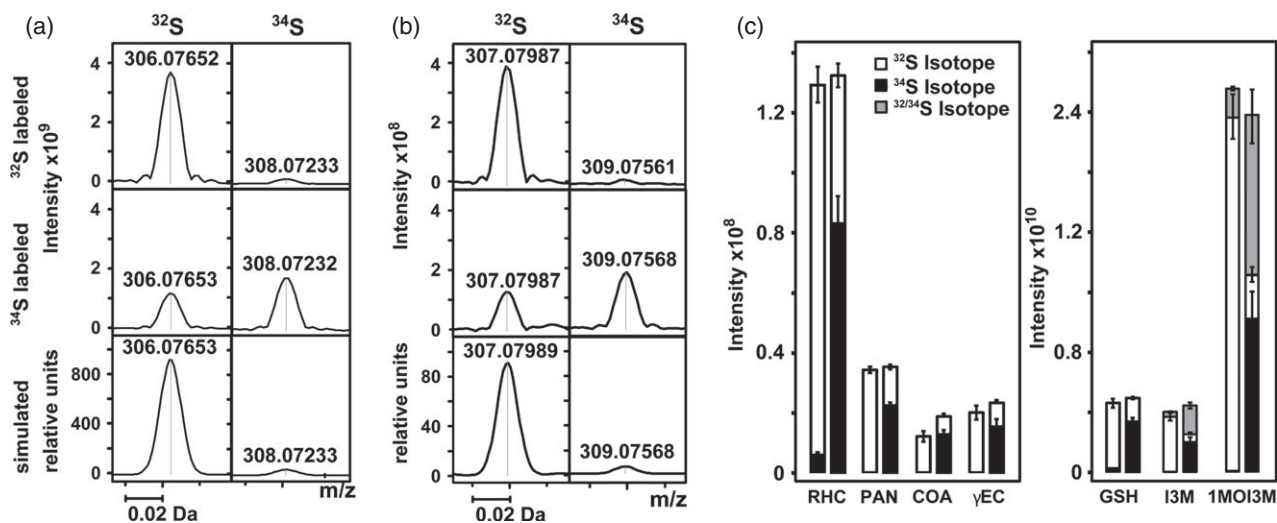
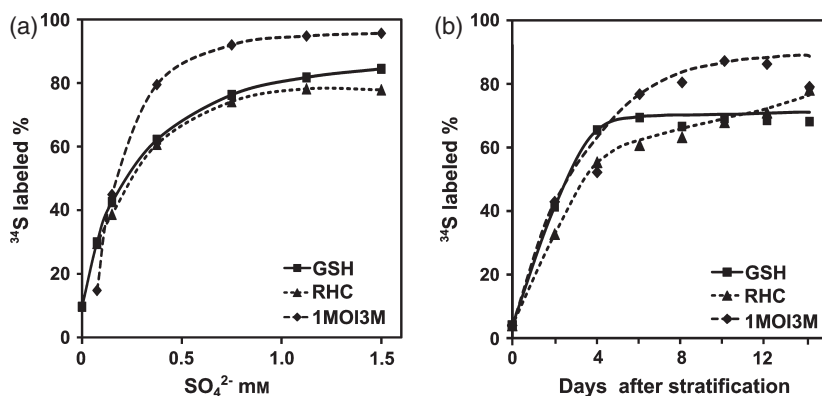


Figure 2. Detection of sulfur compounds in crude extracts of *Arabidopsis thaliana* seedlings by DI-ICR-FTMS in negative ionization mode.

(a) Isotopic mass shift of GSH upon incorporation of either ^{32}S (top) or ^{34}S (middle). The shift of 1.99580 atomic mass units indicative of the ^{34}S monoisotopic compound was observed, as well as the natural abundance of the ^{34}S isotopolog (4%) in the ^{32}S -labeled sample. The simulated isotopolog pattern of GSH (bottom) matches the detected masses within an error ratio of <0.02 ppm.

(b) $^{13}\text{C}_1$ isotope of GSH from the analysis shown in (a). The tenfold lower signal intensity compared to (a) reflects the natural probability of occurrence of ^{13}C per carbon atom in GSH.

(c) Distribution of the ^{32}S (open bars) and ^{34}S (black bars) isotopologs for *S*-ribosyl homocysteine (RHC), pantetheine (PAN), coenzyme A (CoA), γ -glutamyl cysteine (γEC), glutathione (GSH), glucobrassicin (I3M) and neoglucobrassicin (1MOI3M) detected in the samples analyzed in (a); gray bars show the abundance of the hetero-isotopic peaks for compounds containing more than one sulfur.

a linear increase in ^{34}S label occurred from 4% at the start of the feeding experiment, corresponding to the natural abundance of this isotope, to approximately 60% within 4 days for all three sulfur compounds (Figure 1b). After day 6, the labeling efficiency of GSH reached a constant level of approximately 70%, while RHC and 1MOI3M labeling moderately increased to levels of 75 and 90% after 2 weeks, respectively.

In conclusion, the feeding experiments showed efficient incorporation of ^{34}S into three prominent sulfur metabolites. Labeling efficiencies of at least 70% were obtained over a cultivation period of 2 weeks.

The analysis of GSH exemplified the accuracy of the mass spectrometry. The annotated masses of GSH isotopologs were within an error range of 0.05 parts per million

(ppm) for ^{32}S and ^{34}S monoisotopic masses (Figure 2a) and their corresponding ^{13}C isotopes (Figure 2b). The analysis also identified RHC, pantetheine (PAN), coenzyme A (CoA), γEC , glucobrassicin (I3M) and neoglucobrassicin (1MOI3M) on the basis of their isotopic shift, mass accuracy within 0.2 ppm, and peak simulation (Iijima *et al.*, 2008; Nakabayashi and Saito, 2013). The signal intensities of these sulfur compounds in the ICR-FTMS analysis are shown in Figure 2(c) and Figure S1, together with their detected isotopologs in the ^{32}S and ^{34}S labeling experiments. All these sulfur compounds showed the ^{34}S isotopic signal in the range of 50–70% of the sum of isotopolog intensities. The ICR-FTMS signal intensity of distinct masses provides an approximate quantitative read-out (Krajewski *et al.*, 2013). Using GSH, CoA and benzylglucosinolate as standards, we observed a

linear relationship between sulfur compound content and peak intensity in the matrix of the crude extract (Figure S2). The detection limits for GSH, CoA and benzylglucosinolate were 14, 20 and 16 fmol, respectively. The concentrations of GSH and CoA in the extract corresponded to 50 and 7.5 nmol g⁻¹ fresh weight of leaf material provided that no loss occurred during the extraction procedure. The numbers are in agreement with published concentrations of both compounds (May and Leaver, 1993; Mugford *et al.*, 2009).

DI-ICR-FTMS analysis

To achieve highly reproducible spectra, the MS analysis must be optimized with regard to sample dilution, number of scans and ion accumulation time, which have a profound effect on the quality and resolution of the mass spectra (Schmid *et al.*, 2000; Payne *et al.*, 2009). Criteria for selecting the optimal sample dilution are the number of reproducible masses found in the MS analysis and their corresponding mean peak intensity. Analysis of extracts from *Arabidopsis* showed a decrease of reproducibly detected masses from 8000 ion species at 10-fold dilution to approximately 6000 at 100-fold dilution, while peak intensities were not much changed (Figure S3a). The higher the number of accumulated scans, the better the signal intensity, reproducibility and signal-to-noise ratio. However, the sampling time was prolonged (Payne *et al.*, 2009). In order to optimize the number of scans, technical replicates were analyzed at various scan numbers, ranging from 250 to 3000 (Figure S3b). The analysis showed a maximum of almost 12 000 reproducible masses detected at 3000 accumulated scans, and a minimum of approximately 6500 ion species at 250 scans. The number of reproducible ion masses increased only moderately beyond 1000 accumulated scans, with approximately 10 000 different ions detected. Doubling the acquisition time from 1000 to 2000 scans yielded an approximately 10% increase in the number of additional ions identified, with approximately 11 000 ions species. Based on these results, we used 1000 scans per sample and a sample dilution of 1:25 for subsequent analysis of the sulfur metabolome of *Arabidopsis*.

Known sulfur compounds

As a first step in analysis of the MS data generated from *Arabidopsis* extracts, we searched for sulfur-containing metabolites listed in the databases KNApSACk (<http://kana-ya.naist.jp/KNApSACk>), PlantCyc (<http://www.plantcyc.org>) and KEGG (<http://www.genome.jp/kegg>) (Shinbo *et al.*, 2006; Afendi *et al.*, 2012; Altman *et al.*, 2013). The KNApSACk database comprises 626 *Arabidopsis* compounds, including 89 metabolites that contain one to three sulfur atoms in their structure. We found 37 matches that exhibited the sulfur isotope-specific shift, of which ten compounds had not yet been assigned to *Arabidopsis* in the

KNApSACk database (Tables 1 and 2). The listed compounds include prominent low-molecular-weight thiols such as reduced and oxidized GSH, and the related compounds *S*-lactoyl cysteinyl glycine, indol-3-yl methyl GSH and γ EC. In addition, CoA and its derivatives were detected, as well as a large number of glucosinolates, such as I3M, glucoraphanin and glucoerucin (Fahey *et al.*, 2001). The accuracy of the annotated sulfur masses varied between 0.01 and 0.5 ppm in negative ionization mode, and 0.03 and <1.0 ppm in positive ionization mode, with mean deviations from the exact masses of 0.13 and 0.35 ppm, respectively. For example, a prominent sulfur-containing ion had the monoisotopic mass of 447.05379 [M-H]⁻. The sum formula prediction, considering an elemental composition of C₀₋₁₀₀H_nO₀₋₈₀N₀₋₆P₀₋₄S₁₋₃ produced the sum formula C₁₆H₂₀N₂O₉S₂ within the defined accuracy of <0.5 ppm. The sulfur isotope pattern indicated the presence of two sulfur atoms in the compound, as predicted by the sum formula. The analysis perfectly matched the exact mass of the prominent glucosinolate I3M (C₁₆H₂₀N₂O₉S₂) of *Arabidopsis* with a deviation of 0.1 ppm. While the analysis unequivocally identifies a sulfur-containing compound and provides a unique chemical composition in most cases, it does not determine the structure of the compound, and is not able to distinguish between stereoisomers. In summary, our targeted analysis shows that it is possible to detect known low-molecular-weight sulfur compounds.

Untargeted identification of sulfur-containing metabolites

The next task we addressed is the applicability of our approach to identify unassigned sulfur-containing metabolites. Resolution of more than 12 000 ion species in the ICR-FTMS analysis of crude extracts requires efficient filtering tools to identify the molecules of interest. Hierarchical clustering analysis (HCA Hierarchical Clustering Explorer version 3.0; <http://www.cs.umd.edu/hcil/hce>) is one such tool, in which entries from different datasets, generated by differential isotope labeling for example, are compared in a pairwise manner. The HCA selected 1534 ion species from 12 199 reproducible mass signals identified in the negative ionization mode that show low abundance in the ³²S samples and high abundance in the ³⁴S samples (Figure 3a,b). The analysis enriches ion species containing ³⁴S, and includes the reference compounds GSH, PAN, RHC, I3M and 1MOI3M (Figure 3c). The sulfur isotopic mass shift may be used as a second filter. Calculating the isotopic mass shifts for ³⁴S/³²S pairs in the differential labeling experiments reduced the number of HCA-selected ion species to 520. As a third filtering tool, we used prediction of an organic sum formula within the elemental parameters C₀₋₁₀₀H_nO₀₋₈₀N₀₋₆P₀₋₄S₁₋₃, based on a charge of -1 for the measured ion and a maximal deviation of <0.5 ppm from the exact mass. This analysis step reduced the number of sulfur ions to 231. Finally, the isotopic pattern in the spectra

Table 1 Assigned sulfur compounds detected in Arabidopsis extracts by negative ionization (<0.5 ppm)

Sulfur compound	Monoisotopic mass [M-H] ⁻	Detected mass [M-H] ⁻	Charge	Deviation (ppm)	Formula
S-lactoyl cysteinyl glycine; L-γ-glutamyl cysteine	249.05506	249.05505	-1	0.04818	C ₈ H ₁₄ N ₂ O ₅ S
S-ribosyl-L-homocysteine	266.07038	266.07039	-1	0.04510	C ₉ H ₁₇ NO ₆ S
Pantetheine	277.12275	277.12274	-1	0.02887	C ₁₁ H ₂₂ N ₂ O ₄ S
Glutathione disulfide	305.06870	305.06871	-2	0.02950	C ₂₀ H ₃₂ N ₆ O ₁₂ S ₂
Glutathione	306.07653	306.07653	-1	0.01307	C ₁₀ H ₁₇ N ₃ O ₆ S
Dephospho-CoA	342.56716	342.56719	-2	0.08757	C ₂₁ H ₃₆ N ₇ O ₁₆ P ₃ S
CoA	382.55033	382.55027	-2	0.15684	C ₂₁ H ₃₅ N ₇ O ₁₃ P ₂ S
Acetyl CoA	403.55561	403.55579	-2	0.45347	C ₂₃ H ₃₈ N ₇ O ₁₇ P ₃ S
Glucoberverin (3MTP)	406.03056	406.03048	-1	0.20442	C ₁₁ H ₂₁ NO ₉ S ₃
Glucoerucin (4MTB)	420.04621	420.04625	-1	0.08809	C ₁₂ H ₂₃ NO ₉ S ₃
Glucoiberin (3MSOP)	422.02548	422.02568	-1	0.47864	C ₁₁ H ₂₁ NO ₁₀ S ₃
Glucanasturtiin (2PE)	422.05849	422.05828	-1	0.50467	C ₁₅ H ₂₁ NO ₉ S ₂
Glucoberteroin (5MTP)	434.06186	434.06192	-1	0.12901	C ₁₃ H ₂₅ NO ₉ S ₃
Indol-3-yl methyl glutathione	435.13438	435.13438	-1	0.01149	C ₁₉ H ₂₄ N ₄ O ₆ S
Glucoraphanin (4MSOB)	436.04113	436.04118	-1	0.11925	C ₁₂ H ₂₃ NO ₁₀ S ₃
Glucobrassicin (I3M)	447.05374	447.05379	-1	0.10737	C ₁₆ H ₂₀ N ₂ O ₉ S ₂
Glucosquerellerin (6MTH)	448.07751	448.07759	-1	0.16961	C ₁₄ H ₂₇ NO ₉ S ₃
Glucosylsucin (5MSP)	450.05678	450.05685	-1	0.15998	C ₁₃ H ₂₅ NO ₁₀ S ₃
7-methylthioheptyl glucosinolate (7MTH)	462.09316	462.09321	-1	0.09955	C ₁₅ H ₂₉ NO ₉ S ₃
Hydroxyglucobrassicin (1OHIMG, 4OHIMG)	463.04866	463.04865	-1	0.01296	C ₁₆ H ₂₀ N ₂ O ₁₀ S ₂
Glucosperin (6MSOH)	464.07243	464.07249	-1	0.13360	C ₁₄ H ₂₇ NO ₁₀ S ₃
8-methylthiooctyl glucosinolate (8MTO)	476.10881	476.10881	-1	0.00840	C ₁₆ H ₃₁ NO ₉ S ₃
Methoxyglucobrassicin (1MOI3M, 4MOI3M)	477.06431	477.06431	-1	0.00838	C ₁₇ H ₂₂ N ₂ O ₁₀ S ₂
Glucobarin (7MSH)	478.08808	478.08811	-1	0.06693	C ₁₅ H ₂₉ NO ₁₀ S ₃
Glucohirsutin (8MSOO)	492.10373	492.10376	-1	0.06503	C ₁₆ H ₃₁ NO ₁₀ S ₃

Table 2 Assigned sulfur compounds detected in Arabidopsis extracts by positive ionization (<1 ppm)

Sulfur compound	Monoisotopic mass [M-H] ⁺	Detected mass [M-H] ⁺	Charge	Deviation (ppm)	Formula
9-methylthiononanitrile oxide	202.12602	202.12605	+1 M+H	0.17365	C ₁₀ H ₁₉ NOS
S-methyl-5'-thioadenosine	298.09684	298.09683	+1 M+H	0.03388	C ₁₁ H ₁₅ N ₅ O ₃ S
Glutathione	308.09109	308.09105	+1 M+H	0.11685	C ₁₀ H ₁₇ N ₃ O ₆ S
4-methylthiobutylhydroximoyl cysteinylglycine	310.08898	310.08905	+1 M+H	0.23380	C ₁₀ H ₁₉ N ₃ O ₄ S ₂
4-hydroxybutyl glucosinolate	392.06797	392.06826	+1 M+H	0.74655	C ₁₁ H ₂₁ NO ₁₀ S ₂
Benzyl desulfoglucosinolate	353.08981	353.08952	+1 M+Na	0.80999	C ₁₄ H ₁₉ NO ₆ S
5-methylthiopentyl desulfoglucosinolate	379.10883	379.10861	+1 M+Na	0.57213	C ₁₃ H ₂₅ NO ₆ S ₂
3-butenyl glucosinolate	397.04662	397.04650	+1 M+Na	0.30374	C ₁₁ H ₁₉ NO ₉ S ₂
S-adenosyl-L-homocysteine	408.11809	408.11769	+1 M+Na	0.97031	C ₁₄ H ₂₀ N ₆ O ₅ S
Quercetin 3,3'-bissulfate	485.95277	485.95291	+1 M+Na	0.29221	C ₁₅ H ₁₀ O ₁₃ S ₂
Phosphoadenosine-5'-phosphosulfate	530.98273	530.98220	+1 M+Na	0.99306	C ₁₀ H ₁₅ N ₅ O ₁₃ P ₂ S

was re-evaluated with emphasis on the agreement of the number of sulfur atoms in the predicted formula and the pattern of the corresponding sulfur masses. A total of 121 *bona fide* sulfur metabolites were identified, and are listed together with their sum formula in Table S1 and Figure 4(a). The 121 compounds reflect approximately 1.0% of the total ions detected in the analyzed replicates and include the known sulfur metabolites. Thus, approximately 100 unassigned sulfur-containing metabolites were found.

To assess whether filtering by HCA precludes identification of some sulfur metabolites, we omitted HCA and selected only for sulfur isotope-specific mass shifts in the dataset. This approach selected 648 putative sulfur masses out of 12 199 reproducible masses. Subsequent prediction of the chemical composition performed as above selected 306 ion species. Finally, 136 of the selected compounds (1.1%) showed the characteristic isotopic pattern of the 50–70% ³⁴S labeling and the number of sulfur shifts matched the predicted chemical composition. The selected

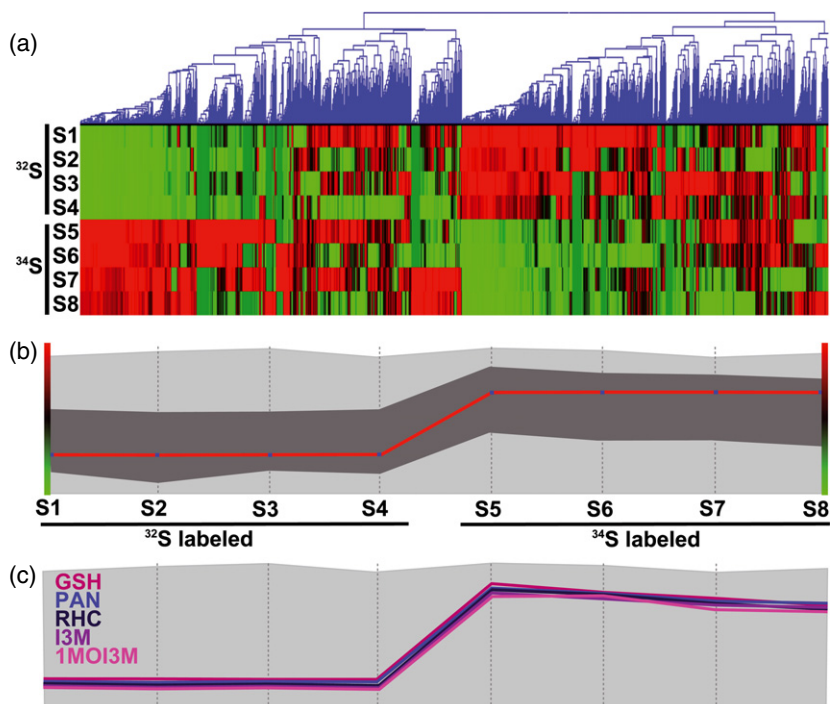


Figure 3. Untargeted analysis for sulfur labeling-specific ions using hierarchical clustering analysis (HCA) on reproducible masses of Arabidopsis extracts. (a) Dendrogram generated from HCA using Euclidean distance measures on mass-spectrometric analyses of Arabidopsis extracts from ^{32}S - and ^{34}S -labeled seedlings (S1–S4 and S5–S8, respectively). The matrix for the analysis was generated within a deviation of 1 ppm, and contained 12 199 reproducible masses. Clusters with high abundance are labeled in red; low abundance groups are labeled in green. (b) HCA profile search based on the clustered masses from (a). ^{34}S -specific masses were selected according to a defined low-to-high profile of signal intensities as indicated by the red line. A total of 1534 ^{34}S sample-specific masses were selected on the basis of a Pearson's correlation coefficient of 0.9 indicated by the dark gray area. (c) Sample profiles of assigned sulfur metabolites identified by HCA as shown in (a) and (b) for glutathione (GSH), pantetheine (PAN), S-ribosyl homocysteine (RHC), glucobrassicin (I3M) and neoglucobrassicin (1MOI3M).

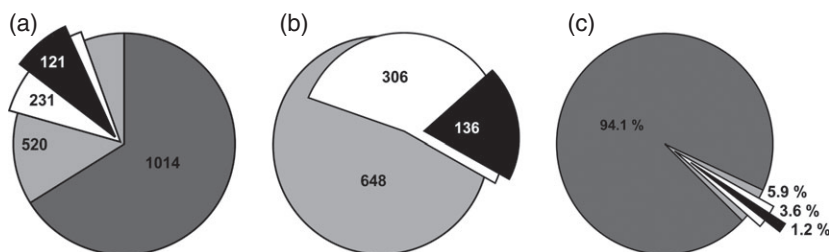


Figure 4. Untargeted identification of sulfur-containing masses in Arabidopsis extracts. (a) A total of 1534 ^{34}S sample-specific masses were selected by HCA from 12 199 reproducible masses. A fraction of 520 ion species show a sulfur isotope-specific mass shift (light gray) and masses without sulfur isotopic mass shift are shown in dark gray. For 231 of these ions (white), the elemental composition with at least one sulfur atom was deduced with <0.5 ppm deviation, and 121 ions (1.0% of the total ions, black) showed the expected pattern of isotope labeling. (b) Identification of putative sulfur masses without HCA on the basis of sulfur isotope-specific mass shifts (648 ions, light gray) and assignment of organic sum formulas (306 ions, white). Of these, 136 ions (1.1% of the total ions, black) showed the characteristic pattern of isotope labeling. (c) Analysis of the abundance of sulfur compounds by random selection of ionic species. One thousand masses ($n = 5$) were randomly picked from the 12 199 reproducible masses, and the mass shift was calculated for one to three ^{34}S atoms. Masses without sulfur isotope pattern are presented as dark gray fraction. The percentage of ion species with such a shift is shown in light gray (5.9%). Visual analysis of the spectra for the labeling-specific fingerprint reduced the number of sulfur-containing ions to 3.6% ($\pm 0.6\%$; white). Elemental composition was assigned to $1.2 \pm 0.2\%$ among the thousand selected masses (black).

fraction comprised all 121 compounds identified by the first clustering approach and 15 additional compounds, which were discarded by HCA because of low signal intensities and low statistical significance (Figure 4b and Table S1).

Both filtering approaches resulted in assignment of 1.0–1.1% of mono-charged and non-isotopic ions of sulfur compounds among all ions identified in the Arabidopsis crude extract. We wished to determine how many sulfur compounds were overlooked by our data analysis

methods. To do this, we performed a control analysis by selecting randomly 1000 ions ($n = 5$) from the previous analysis and 'hand-selecting' the sulfur candidates. All the unbiased chosen peaks were analyzed for possible sulfur isotope pairs in the $^{32}\text{S}/^{34}\text{S}$ experiments by calculating the mass shift and comparing the list of recorded ion masses. A total of $5.9 \pm 0.6\%$ of the analyzed ionic species fulfilled the criterion. The number was reduced to $3.6 \pm 0.6\%$ after analysis of the isotope pattern in the ICR-FTMS spectra. We conclude that a maximum of 3.6% of the detected mass ions contain sulfur in their chemical composition. Among those ions are isotopologs and ionization adducts. In fact, a single metabolite may generate a family of associated ion masses (Draper *et al.*, 2009; Krueve *et al.*, 2013). Therefore, calculation of the organic sum formula is a necessary step towards identifying the number of different metabolites, despite the possibility that the assumed organic composition is too restrictive and excludes some sulfur compounds. Application of the sum formula calculation yielded $1.2 \pm 0.2\%$ sulfur-containing metabolites among the randomly chosen ion species (Figure 4c). The value closely matched the previous values of 1.0 and 1.1%, and gives credence to the efficiency of the two filtering methods used. In addition, when the Arabidopsis extracts were analyzed in positive ionization mode, analysis of the data by HCA, sulfur shift and elemental composition yielded 55 additional sulfur masses of which two are known and 53 are uncharacterized (Table S2).

Identification and analysis of mutant-related masses

The filtering tools provide a solid base to identify sulfur compounds in an untargeted manner. Endogenous targets of the vacuolar γ -glutamyl transferase GGT4, which is involved in GSH and GS conjugate turnover, have not been described to date. We applied the sulfur-labeling strategy to analyze the *ggt4-1* knockout line with the aim of identifying endogenous GS conjugates or related compounds that may accumulate in the mutant because of the GGT4 deficiency. Arabidopsis seedlings of the mutant and parental *Ler-0* line were examined for changes in sulfur-containing metabolites by S-calc analysis (see experimental procedures) and HCA. Fourteen sulfur-containing ion species with specifically altered levels in the mutant were identified (Figure 5). Seven of these compounds were either uniquely detected in the *ggt4-1* sample or highly enriched in the mutant by a factor ranging from approximately fivefold for the ion at 362.1027 [M-H]⁻ to 130-fold for the ion at 490.0903 [M-H]⁻ compared to wild-type (Figure 5a). The signals for a number of sulfur compounds, including RHC, decreased in intensity in *ggt4-1* extracts (Figure 5b). Other sulfur-containing compounds such as PAN, GSH and 1MOI3M had levels comparable to the wild-type (Figure S4).

γ -glutamyl transferases are specific for the transfer of γ -glutamyl groups from peptides such as GSH (Martin

et al., 2007). Thus, the identified mutant-specific compounds may be γ -glutamyl-containing sulfur metabolites such as GSH-derived compounds. To explore this possibility, we used an enzymatic assay to detect the presence of a γ -glutamyl group, and used MS/MS fragmentation analysis to further characterize the metabolites.

First, plant extracts and a GSH solution were incubated with purified GGT, and the samples were subsequently analyzed by mass spectrometry. The analysis clearly showed a GGT- and time-dependent turnover of GSH and the 452.1346 [M-H]⁻ and 502.1051 [M-H]⁻ compounds, while 1MOI3M, which contains no γ -glutamyl group, is unaltered by incubation with the GGT (Figure 6a). This finding indicated that both accumulated metabolites contain a γ -glutamyl moiety.

In a second line of experimentation, MS/MS fragmentation analysis was applied. We focused on the specifically accumulated ion that showed the highest intensity in the *ggt4-1* mutant (452.1346 [M-H]⁻) and the corresponding ^{34}S isotopolog, which were approximately tenfold enriched in the mutant (Figure 5a). The fragmentation pattern showed single ions at 306.076 [M-H]⁻ and 308.072 [M-H]⁻, respectively, matching the monoisotopic masses of GSH and the ^{34}S isotopolog (Figure 6b). The 146.058 [M-H]⁻ cleaved-off fragment has the predicted elemental composition of $\text{C}_6\text{H}_{10}\text{O}_4$ (0.7 ppm) and was not detected in the analysis. The fragmentation of this group probably occurred as a neutral loss accompanied by a proton shift from the conjugated group to the glutathione moiety, which induces an intramolecular rearrangement of the group (Kanawati *et al.*, 2011). Thus, the original conjugated group in the neutral GS conjugate has a sum formula of $\text{C}_6\text{H}_{11}\text{O}_4$. In conclusion, the analysis revealed a γ -glutamyl-containing sulfur compound comprising a moiety of the exact mass and elemental composition of GSH, in addition to a $\text{C}_6\text{H}_{10}\text{O}_4$ fragment.

The deficiency in vacuolar GGT function of the *ggt4-1* mutant is expected to result in higher abundances of GGT4 substrates such as GS conjugates and reduced levels of subsequent breakdown products such as cysteinyl or cysteinyl glycine conjugates (Ohkama-Ohtsu *et al.*, 2007b; Blum *et al.*, 2010). Hence, we evaluated the possibility that other mass signals specifically enriched in the mutant may indicate GS-conjugates and those with reduced signals possible catabolites thereof. Indeed, six predicted GS conjugates accumulated in *ggt4-1* while the corresponding Cys conjugate showed a decreased level (Figure 7). The $\text{C}_6\text{H}_{11}\text{O}_4$ GS conjugate previously described has a corresponding Cys conjugate that is 2.2-fold reduced in the mutant and is isomeric with RHC. In addition, we were able to assign several other conjugated groups, including $\text{C}_4\text{H}_5\text{O}_4$ and $\text{C}_6\text{H}_{11}\text{O}_5$, which possibly represent dicarboxyethyl and glucopyranosyl conjugates. To corroborate this finding, the independent *ggt4-2* knockout line generated in the Col-0 background was also analyzed (Figure 7). The

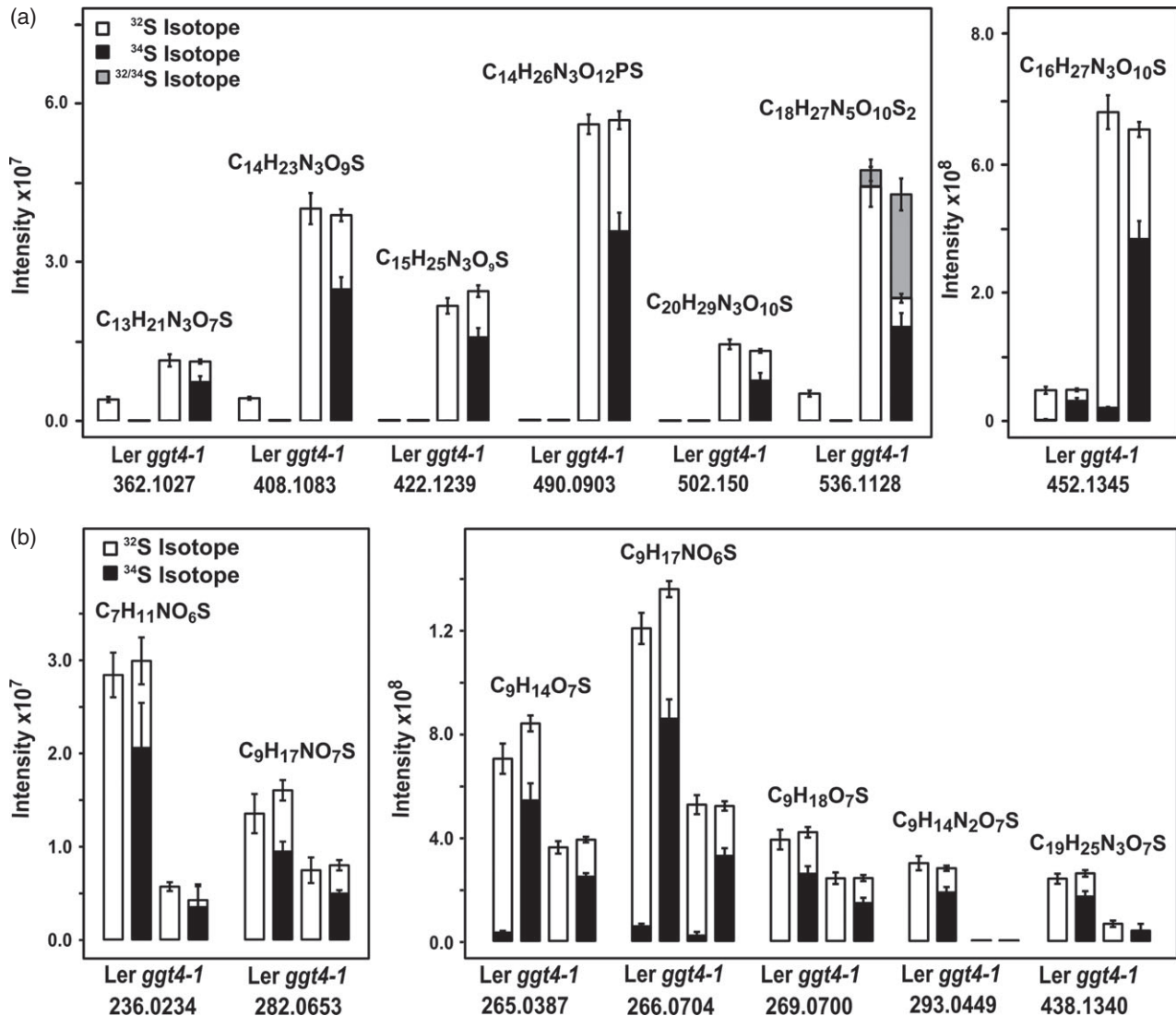


Figure 5. Analysis of the *ggt4-1* mutant for altered sulfur masses.

The selected masses were identified by differential comparison of sulfur-containing masses between *ggt4-1* and the parental line. The predicted neutral elemental composition is shown, with a maximal deviation from the exact mass <0.5 ppm.

(a) Mass signals that accumulate in *ggt4-1*. The signal intensity and isotope distribution of the altered mutant masses for the ^{32}S -labeled sample (left bar) and the ^{34}S -labeled sample (right bar) are shown.

(b) Mass signals that are specifically reduced in *ggt4-1*. The intensities of ion species in the mutant and the parental line are shown (see above).

sulfur metabolite changes observed were in full agreement with the previous results, and showed that the alterations are a consequence of GGT4 deficiency.

DISCUSSION

High-resolution mass spectrometry, in combination with stable isotope-labeling, has revolutionized analysis of the proteome and metabolome (Smith, 2000; Allwood *et al.*, 2012). In this study, we applied ultra-high-resolution mass spectrometry using DI-ICR-FTMS and sulfur labeling for an analysis of the sulfur metabolome of *Arabidopsis thaliana*. This high resolution enables us to analyze complex samples containing a multitude of metabolites without

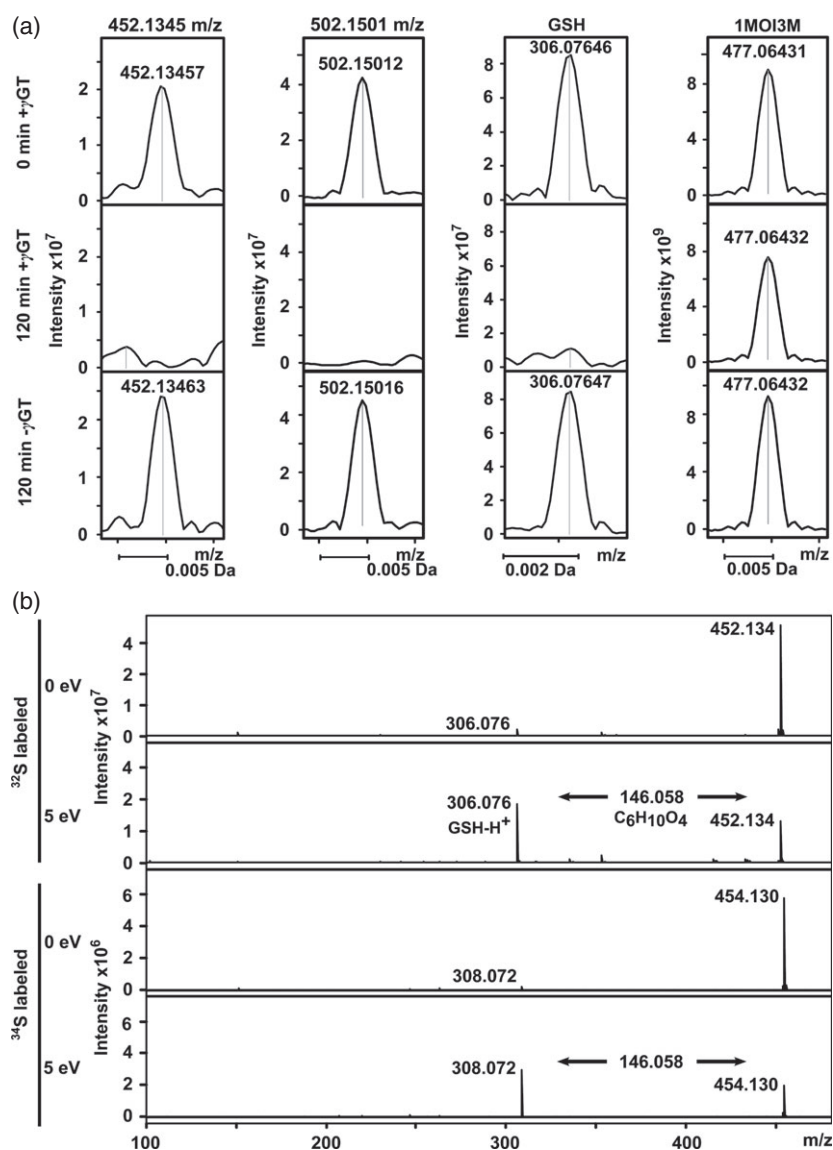
prior chromatographic separation. The mass accuracy achieved allows assignment of unique elemental compositions to the organic ions (Hegeman *et al.*, 2007; Matsuda *et al.*, 2009; Saito and Matsuda, 2010).

The reproducibility and comparability of the analysis are critical for identification of metabolites that are selectively enriched in samples by using an untargeted approach (Saito and Matsuda, 2010). Recently, ^{34}S labeling was introduced for metabolome analysis using online liquid chromatography and high-resolution MS (Giavalisco *et al.*, 2011; Hsieh *et al.*, 2012). The studies identified sulfur-containing metabolites in *Arabidopsis* based on the labeling-specific isotopic pattern. Giavalisco *et al.* (2011)

Figure 6. Analysis of sulfur compounds that specifically accumulate in the *ggt4-1* mutant.

(a) Turnover of sulfur compounds with mass 452.1345 [M-H]⁻ and 502.1501 [M-H]⁻ by γ -glutamyl transferase. The compounds and GSH are specifically catabolized by the action of the γ -glutamyl transferase (compare signals at incubation times 0 and 120 min). Neoglucobrassicin (right; 1MOI3M), which contains no γ -glutamyl group, is unaffected by the enzymatic action. Incubation without GGT served as a control (bottom row).

(b) Fragmentation analysis of the unknown compound C₁₆H₂₆O₁₀N₃S. The compound with mass 452.1345 [M-H]⁻ was fragmented by collision with argon. The fragmentation pattern is shown for the ³²S-labeled compound (row 2) and the ³⁴S-labeled compound (row 4). Rows 1 and 3 show the mass signals detected prior to collision. The major fragments have exact masses of 306.07639 *m/z* and 308.07211 *m/z* and match the monoisotopic masses of GSH with errors of 0.3 and 0.7 ppm, respectively. The mass difference compared with the original mass is 146.05784 atomic mass units for both the ³²S- and ³⁴S-labeled samples, which indicates a leaving group consisting of C₆H₁₀O₄ (<0.4 ppm).



demonstrated the feasibility of assigning unique sum formulas to such compounds by a multiple labeling approach. Our study shows that a single labeling approach with sulfur is sufficient for annotating sum formulas to low molecular sulfur masses in most cases (>80%). Hsieh *et al.* (2012) used LC-MS and positive ionization for quantification of prominent sulfur compounds such as GSH in plant extracts. However, the capability for sulfur metabolite detection in a targeted or untargeted manner was not explored. The online MS analysis does not capitalize on major advantages provided by ICR-FTMS, which include enhanced sensitivity and an increase in the number of resolved ion species by increasing the number of scans per acquisition (Payne *et al.*, 2009).

In our untargeted approach, we wished to detect soluble, low-molecular-weight sulfur compounds to study

endogenous GSH-derived metabolites. To this end, methanolic extracts of *Arabidopsis* seedlings were analyzed without further chromatography to minimize loss of compounds. The approach allowed assignment of 37 sulfur metabolites listed in the databases, including a number of glucosinolates, which show development-specific abundances in *Arabidopsis* (Petersen *et al.*, 2002; Brown *et al.*, 2003). Furthermore, we identified 167 sulfur-containing metabolites not listed in accessible databases, which are *bona fide* sulfur-containing molecules from *Arabidopsis* based on three criteria: the presence of a ³⁴S labeling-induced isotopic shift in sulfur-containing masses, the presence of the ¹³C₁ isotopic peak and its ³⁴S isotopolog, and unequivocal assignment of the elemental composition for a sulfur-containing organic compound within <0.5 ppm accuracy.

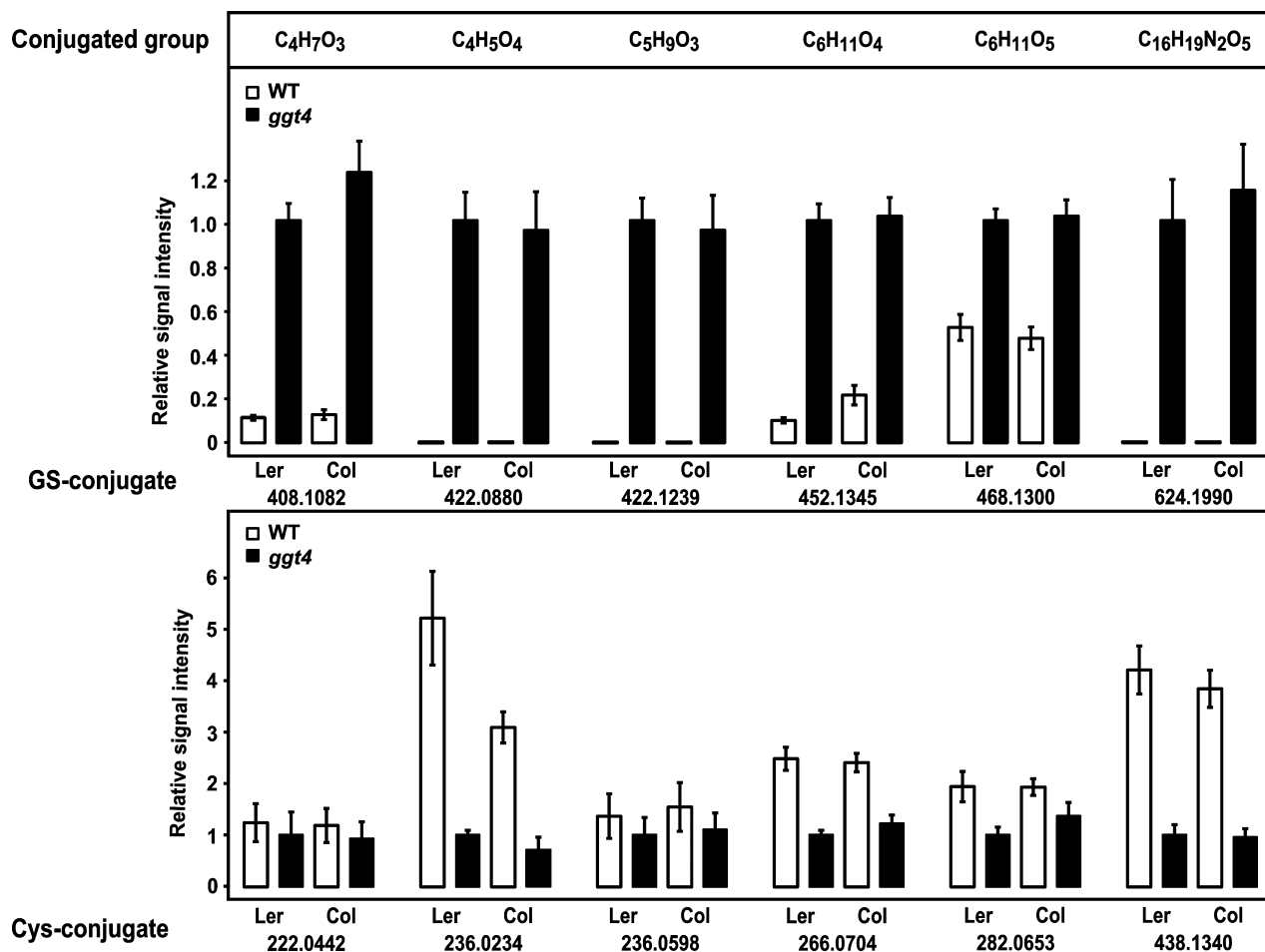


Figure 7. Prediction of putative GS conjugates with altered abundance in GGT4 knockout mutants.

Two independent allelic GGT4 mutants in the Ler-0 and Col-0 background were analyzed. The upper diagram shows the relative signals for the ^{32}S species for the postulated GS conjugates of the parental lines (open bars) and the GGT4 mutants (black bars). The lower diagram shows the signals for the expected Cys conjugates. The elemental composition of the deduced conjugated moiety is shown above. The variation of the mass signals is expressed as relative signal intensities (mean \pm SD) with respect to the specific GS conjugate signal in *ggt4-1* (Ler-0 background).

The prime criterion for identification of sulfur compounds is the isotopic shift, which is sometimes difficult to determine because of numerous peaks of similar ionic mass, especially in regions of high ion density. Our experience in this study has been that half-saturating ^{34}S labeling generates a specific signature, reducing the ^{32}S signal and enhancing the ^{34}S signal to an approximately each other level. This signature facilitates recognizing sulfur-labeled masses compared to the pattern generated complete isotopic labeling. In addition, the half-saturating condition permits identification of compounds with more than one sulfur atom because of the sulfur isotope heteromeric pattern. Thus, the partial labeling approach helps to determine the number of sulfur atoms in the molecule and supports formula assignment.

Recently, Nakabayashi *et al.* (2013) described an untargeted metabolomic approach to identify sulfur metabolites in onion bulbs. The study used ^{13}C labeling and the natural

abundance of ^{34}S (approximately 4%) together with a visual identification strategy to annotate the sulfur compounds. The strategy is successful with abundant sulfur-containing metabolites and in less complex plant extracts. However, the natural abundance of ^{34}S is frequently insufficient to allow clear assignment of less prominent metabolites when an induced shift of sulfur-containing masses is lacking. Generally, stable isotope labeling contributes profoundly to formula assignment and further structural elucidation (Kind and Fiehn, 2006). A stable isotope labeling strategy was used in the study by Giavalisco *et al.*, (2011) using chromatographic separation of Arabidopsis extracts prior to FTMS analysis. The analysis led to the detection of 40 sulfur metabolites listed in the KNApSACK database for Arabidopsis. Our approach revealed 37 known sulfur metabolites, of which 21 overlapped with the Giavalisco study.

The methanolic extraction procedure used in our study favors the recovery of polar sulfur metabolites, allowing

detection and analysis of GSH and related compounds (Liao *et al.*, 2012; Krajewski *et al.*, 2013). There are approximately 300 sulfur metabolites assigned to the Arabidopsis metabolome in the KNApSACk, PlantCyc and KEGG databases. Most of these sulfur metabolites were not detected in the analysis by Giavalisco *et al.* (2011) or in our study. There are a number of reasons why these compounds were not recovered. Sample preparation and fractionation greatly influences metabolite presence and detection capacity. We used seedlings grown under continuous light and an aqueous extraction solvent of 70% methanol, which recovered mostly polar compounds (Li *et al.*, 2007). Furthermore, inefficient ionization or ion suppression caused by the matrix may affect detection of metabolites (Ohta *et al.*, 2010). In addition, environmental and developmental parameters strongly alter the concentrations of compounds in the plant material, such as glucosinolates and camalexin, that are induced upon pathogen infection (Glazebrook and Ausubel, 1994; Brown *et al.*, 2003; Bednarek *et al.*, 2011; Joosen *et al.*, 2013).

The major benefit of the differential labeling approach is comparative analysis. Biological samples reflecting different stages of development, environmental conditions or genotypes (including accessions and mutants) may be compared. The analysis tools used in this study allow efficient data processing for detection of specific changes in the sulfur metabolome. Recent studies have implicated GSH as a sulfur donor in the biosynthesis of glucosinolates (Sønderby *et al.*, 2010). The presumed GS conjugate of the glucosinolate precursor must be trimmed by removal of the γ -glutamyl moiety. The GGT activity provides the enzymatic activity for this postulated step. The vacuolar GTT4 is involved in GS conjugate turnover (Grzam *et al.*, 2007; Ohkama-Ohtsu *et al.*, 2007b). Endogenous substrates of GGT4 other than from GSH and the involved pathways are not yet known. Neither the *ggt4-1* mutant nor double and triple mutants in combination with Δ PCS1, Δ PCS2, *ggt1* or *ggt2* mutations show an altered phenotype in addition to the slight progressive senescence that was observed for GGT1 mutants (Martin *et al.*, 2007; Ohkama-Ohtsu *et al.*, 2007a; Destro *et al.*, 2011). Thus, changes in the metabolite profile caused by GGT4 deficiency offer indications as to the function of this enzyme in plant metabolism. Our analysis revealed several sulfur compounds that are specifically enriched or reduced in the *ggt4-1* mutant. Among the sulfur compounds enriched in *ggt4-1* were a number of predicted GS conjugates. We provide enzymatic evidence that two of the compounds contained a γ -glutamyl group. One of the compounds has been characterized as a GS conjugate with a predicted C₆H₁₁O₄ group attached. The sum formula of this moiety is compatible with a number of structures, including aliphatic carboxylic acids or deoxy sugars, that may be conjugated to GSH. Structural elucidation of this moiety is a challenge for the future, and

requires enrichment of the compound, purification and subsequent NMR analysis (Nakabayashi and Saito, 2013). The accumulation of a GS conjugate due to decreased turnover is expected to be accompanied by reduced levels of further breakdown products. Consistent with this hypothesis, we assigned five more GS conjugates and the respective cysteinyl conjugates to the sulfur metabolome of Arabidopsis. Corresponding cysteinyl glycine conjugates were not detected, due to low endogenous levels and rapid degradation to Cys conjugates by carboxypeptidases, such as phytochelatin synthase (Blum *et al.*, 2007; Ohkama-Ohtsu *et al.*, 2008; Geu-Flores *et al.*, 2009).

The dicarboxyethyl GSH found in this study has not been described previously in plants. It is formed in vertebrates by conjugation of GSH to malate (Tsuboi *et al.*, 1990). Its role is still not fully elucidated, but it has an inhibitory effect on blood coagulation and platelet aggregation, probably involving adenylate cyclase (Tsuboi *et al.*, 1993). Dicarboxyethyl GSH has been proposed as an intermediate in detoxification of reactive aldehydes generated by oxidation of fatty acids (Singh *et al.*, 2006). Aldehydes, including sugars in their aldose conformation, are common targets of glutathionylation in animal and plant systems, for example in the glyoxylate pathway (Sousa Silva *et al.*, 2013; Stewart *et al.*, 2013). Thus, some of the predicted GS conjugates altered in the *ggt4-1* mutant may be related to sugar metabolism and involved in oxidative stress responses.

CONCLUSIONS

More than 150 sulfur compounds and their elemental compositions that have not yet been listed in databases were described in this study. This finding emphasizes the analytical power of the approach and the need for a more detailed understanding of the Arabidopsis sulfur metabolome. A broad range of sulfur metabolites may be analyzed by DICR-FTMS and stable sulfur isotope labeling. The analysis allows to identify changes in the metabolism of sulfur compounds imposed by environmental cues or altered genotypes. Furthermore, the approach facilitates assigning the elemental compositions to the sulfur compounds. The approach has great promise for elucidation of endogenous GS conjugates and their biosynthetic as well as catabolic routes in plants. In addition, the methods we have established may open up new avenues of research in terms of assessing dynamic changes in the sulfur metabolome in response to developmental, environmental, biotic and abiotic signals.

EXPERIMENTAL PROCEDURES

Plant material

A. thaliana lines were obtained from the Nottingham Arabidopsis Stock Centre (<http://arabidopsis.info/>). The lines included Columbia (Col-0), Landsberg *erecta* (Ler-0), and the GGT4 knockout lines

ggt4-1 (stock number N161036; *Ler-0* background; Ohkama-Ohtsu et al., 2007b) and *ggt4-2* (GK-631A04; Col-0 background; <http://www.gabi-kat.de>; Ohkama-Ohtsu et al., 2011).

Heavy isotope labeling and plant growth conditions

The isotope labeling of *Arabidopsis* was performed using a modified sulfur-free MS medium (Sauter et al., 2004). The solidified medium (0.9% w/v agar) was supplemented with 0.36 mM Na₂³²SO₄ or Na₂³⁴SO₄, and seedlings were grown for 2 weeks under continuous light unless otherwise stated. Elemental ³⁴S of 99.9% purity was obtained from Isoflex USA (<http://www.isoflex.com>). The sulfur (pure ³⁴S, or ³²S with 4% natural content of ³⁴S) was converted to SO₂ under pure oxygen atmosphere. Subsequently, the gas was introduced into an aqueous solution of 0.2 M NaOH containing 10% H₂O₂ for oxidation to Na₂SO₄, and the solution was subsequently neutralized with 1 M hydrochloric acid. The solution was dried at 60°C, and the yield of Na₂SO₄ was in the range of 90%. All chemicals used were of analytical grade.

Metabolite extraction

Two-week-old seedlings were collected from agar plates, washed in water, dried on paper towels, and frozen in liquid nitrogen. Seedlings were stored in 0.1 g aliquots at -80°C until extraction. The frozen seedlings were homogenized using a glass pestle in Eppendorf tubes. The ground plant material was extracted in methanolic solution and sonicated for each extraction step. The first extraction was performed using 50% methanol/water, 0.1% formic acid (0.25 ml), and the second was performed using 100% methanol/water, 0.1% formic acid (0.25 ml). Ultrasonication was performed at 85% intensity for 20 sec (Sonopuls; Bandelin, <http://www.bandelin.com>). After each extraction step, the debris was sedimented by centrifugation (20 000 g, 30 min, 4°C). Supernatants were combined and stored at -80°C. The samples were prepared 1 day prior to MS analysis.

DI-ICR-FTMS

Ultra-high-resolution mass spectra were acquired using an ICR-FT mass spectrometer (Solarix; Bruker Daltonics, <http://www.bruker.com>) equipped with a 12 T superconducting magnet (Magnex Scientific/Varian Inc., <http://www.agilent.com>) and an electron spray source (Apollo II; Bruker Daltonics). Measurements and external calibration were performed as described by Janz et al. (2010). The spectra were recorded for an *m/z* range of 123–1000, with an ion accumulation time of 0.3 msec. Metabolite extracts were routinely diluted 1:25 in 70% methanol/water (Lichrosolv; Sigma-Aldrich, <http://www.sigmaaldrich.com>) prior to analysis. We used at least four biological replicates per genotype, two for each labeling condition, and assayed each biological sample twice (technical replicates). ICR-FTMS spectra were calibrated internally by using the exact masses of known metabolites: all aliphatic fatty acids from C₁₂ to C₂₄, and the sulfur-containing compounds γEC, GSH and 1MOI3M. Calibration was performed using data analysis software (Bruker Daltonics) with an accuracy of 0.05 ppm, and exported to peak lists at a signal to noise ratio of 4 containing the spectral information of mass and corresponding intensity.

Hierarchical clustering analysis

Reproducible mass signals were identified by HCA using Hierarchical Clustering Explorer version 3.0 (<http://www.cs.umd.edu/hcil/hce>). The clustering and model-based profile search were performed using a Pearson's correlation coefficient of 0.9 (Janz et al., 2010).

Prediction of sulfur-containing ions by isotopic mass shift

Possible sulfur-containing masses were selected based on two equations:

$$0 < [\text{mass}_i^{32\text{S}}]_{34\text{S}} < [\text{mass}_i^{32\text{S}}]_{32\text{S}} \quad (1)$$

in which the term in brackets signifies the signal intensity of a specific mass *i* of the ³²S isotope in the ³⁴S- and ³²S-labeled samples, and

$$[\text{mass}_i^{32\text{S}}]_{34\text{S}} < [\text{mass}_i^{34\text{S}}]_{34\text{S}} \quad (2)$$

which refers the signal intensity of ³²S and ³⁴S isotopologs within the ³⁴S-labeled sample. These equations were applied in the filtering process (S-CALC) by using Matlab (<http://www.mathworks.de>). The mass shift was calculated for one to three sulfur atoms in the compound at <1 ppm accuracy.

Sum formula annotation to sulfur masses

Organic sum formulas were assigned for monoisotopic masses with an elemental composition in the range C₀₋₁₀₀H_nO₀₋₈₀N₀₋₆P₀₋₄S₁₋₃ and a charge of -1 using the Formulae 1.2 Megapeak program (M. Frommberger, Helmholtz Zentrum, Munich, Germany; Hertkorn et al., 2008; Herzprung et al., 2010). Isotopic masses for ³⁴S₁₋₃ and ¹³C₁ and ionization adducts were excluded from the formula calculation. Formula predictions were accepted at a maximal deviation of the calculated and measured masses of 0.5 ppm. Equally likely compositional assignments were selected based on their probability by applying the method for sum formula verification established by Kind and Fiehn (2007).

Fragmentation analysis

Cell-free extracts from *Arabidopsis* seedlings (0.8 g, 4 ml) were freeze dried and re-suspended in 4 ml water prior to solid-phase extraction using a C18 column (Bakerbond SPE C18, 1000 mg, 6 ml; J.T. Baker, Netherlands, <http://www.jtbaker.nl/>). Elution was performed using 0, 2, 4, 6, 10 and 15% acetonitrile in water (2 ml). Fractions were freeze-dried and dissolved in 0.5 ml of 70% methanol for analysis. The eluate enriched in the compound of interest was chosen for further analysis (4% acetonitrile fraction for 452.1345 [M-H]⁻ from the *ggt4-1* mutant). The MS/MS analysis was performed as described previously using an ion accumulation time of 10 sec per scan (von Saint Paul et al., 2011).

Analysis of γ-glutamyl residues

Freeze-dried metabolite fractions were dissolved in 0.5 ml buffer (10 mM Tris/HCl, pH 8), and 0.1 ml of the solution was incubated with equine GGT (4 × 10⁻³ units in 0.2 μl buffer; Sigma-Aldrich) at 37°C for 2 h, essentially as described by Tate and Meister (1985). Freshly prepared GSH solution (10 μM in buffer) and incubations without enzyme administration served as controls. The reaction was stopped by adding 10% formic acid in water to a final concentration of 0.1%. The samples were immediately stored at -80°C and prepared 1 day prior to ICR-FTMS analysis.

ACKNOWLEDGEMENTS

We are grateful to Farhah Assaad and Alexander Christmann for critical reading of the manuscript, and to Erich Glawischnig (Lehrstuhl für Genetik, TU München) for providing the benzyl glucosinolate standard. We thank the Deutsche Forschungsgemeinschaft for financial support (grant number DFG EG938/4).

SUPPORTING INFORMATION

Additional Supporting Information may be found in the online version of this article.

Figure S1. Mass shift of assigned sulfur compounds found in *Arabidopsis* extracts.

Figure S2. Quantitative analysis of sulfur compounds by ICR-FTMS.

Figure S3. Optimization of ICR-FTMS sample analysis.

Figure S4. Unaltered sulfur metabolites of the parental line (Ler-0) and the *ggt4-1* mutant.

Table S1. Validated sulfur-containing masses detected by negative ionization.

Table S2. Validated sulfur-containing masses detected by positive ionization.

REFERENCES

- Afendi, F.M., Okada, T., Yamazaki, M. *et al.* (2012) KNApSACk family databases: integrated metabolite-plant species databases for multifaceted plant research. *Plant Cell Physiol.* **53**, e1.
- Agerbirk, N. and Olsen, C.E. (2012) Glucosinolate structures in evolution. *Phytochemistry*, **77**, 16–45.
- Allwood, J.W., Parker, D., Beckmann, M., Draper, J. and Goodacre, R. (2012) Fourier transform ion cyclotron resonance mass spectrometry for plant metabolite profiling and metabolite identification. *Methods Mol. Biol.* **860**, 157–176.
- Altman, T., Travers, M., Kothari, A., Caspi, R. and Karp, P.D. (2013) A systematic comparison of the MetaCyc and KEGG pathway databases. *BMC Bioinformatics*, **40**, 112.
- Beck, A., Lenzian, K.J., Oven, M., Christmann, A. and Grill, E. (2003) Phytochelatin synthase catalyzes key step in turnover of glutathione conjugates. *Phytochemistry*, **62**, 423–431.
- Bednarek, P., Piślewska-Bednarek, M., Ver Loren van Themaat, E., Maddula, R.K., Svatoš, A. and Schulze-Lefert, P. (2011) Conservation and clade-specific diversification of pathogen-inducible tryptophan and indole glucosinolate metabolism in *Arabidopsis thaliana* relatives. *New Phytol.* **132**, 713–726.
- Blake-Kalff, M.M.A., Harrison, K.R., Hawkesford, M.J., Zhao, F.J. and McGrath, S.P. (1998) Distribution of sulfur within oilseed rape leaves in response to sulfur deficiency during vegetative growth. *Plant Physiol.* **118**, 1337–1344.
- Blum, R., Beck, A., Korte, A., Stengel, A., Letzel, T., Lenzian, K.J. and Grill, E. (2007) Function of phytochelatin synthase in catabolism of glutathione-conjugates. *Plant J.* **49**, 740–749.
- Blum, R., Meyer, K.C., Wünschmann, J., Lenzian, K.J. and Grill, E. (2010) Cytosolic action of phytochelatin synthase. *Plant Physiol.* **153**, 159–169.
- Böttcher, C., Westphal, L., Schmotz, C., Prade, E., Scheel, D. and Glawischning, E. (2009) The multifunctional enzyme CYP71B15 (PHYTOALEXIN DEFICIENT3) converts cysteine-indole-3-acetonitrile to camalexin in the indole-3-acetonitrile metabolic network of *Arabidopsis thaliana*. *Plant Cell*, **21**, 1830–1845.
- Brown, P.D., Tokuhisa, J.G., Reichelt, M. and Gershenzon, J. (2003) Variation of glucosinolate accumulation among different organs and developmental stages of *Arabidopsis thaliana*. *Phytochemistry*, **62**, 471–481.
- Buchner, P., Stuver, C.E.E., Westerman, S., Wirtz, M., Hell, R., Hawkesford, M.J. and de Kok, L.J. (2004) Regulation of sulfate uptake and expression of sulfate transporter genes in *Brassica oleracea* as affected by atmospheric H₂S and pedospheric sulfate nutrition. *Plant Physiol.* **136**, 3396–3408.
- Creek, D.J., Chokkathukalam, A., Jankevics, A., Burgess, K.E.V., Breitling, R. and Barrett, M.P. (2012) Stable isotope-assisted metabolomics for network-wide metabolic pathway elucidation. *Anal. Chem.* **84**, 8442–8447.
- Cummins, I., Dixon, D.P., Freitag-Pohl, S., Skipsey, M. and Edwards, R. (2011) Multiple roles for plant glutathione transferases in xenobiotic detoxification. *Drug Metab. Rev.* **43**, 266–280.
- Davoine, C., Falletti, O., Douki, T., Iacazio, G., Ennar, N., Montillet, J.-L. and Triantaphylidès, C. (2006) Adducts of oxylipin electrophiles to glutathione reflect a 13 specificity of the downstream lipoxygenase pathway in the tobacco hypersensitive response. *Plant Physiol.* **140**, 1484–1493.
- Destro, T., Prasad, D., Martignago, D., Bernet, I.L., Trentin, A.R., Renu, I.K., Ferretti, M. and Masi, A. (2011) Compensatory expression and substrate inducibility of gamma-glutamyl transferase GGT2 isoform in *Arabidopsis thaliana*. *J. Exp. Bot.* **62**, 805–814.
- Dixon, D.P. and Edwards, R. (2009) Selective binding of glutathione conjugates of fatty acid derivatives by plant glutathione transferases. *J. Biol. Chem.* **284**, 21249–21256.
- Dixon, D.P., Skipsey, M. and Edwards, R. (2010) Roles for glutathione transferases in plant secondary metabolism. *Phytochemistry*, **71**, 338–350.
- Draper, J., Enot, D.P., Parker, D., Beckmann, M., Snowdon, S., Lin, W. and Zubair, H. (2009) Metabolite signal identification in accurate mass metabolomics data with MZedDB, an interactive *m/z* annotation tool utilising predicted ionisation behaviour 'rules'. *BMC Bioinformatics*, **10**, 227.
- Edwards, R. and Dixon, D.P. (2005) Plant glutathione transferases. *Methods Enzymol.* **401**, 169–186.
- Fahey, J.W., Zalcmann, A.T. and Talalay, P. (2001) The chemical diversity and distribution of glucosinolates and isothiocyanates among plants. *Phytochemistry*, **56**, 5–51.
- Geu-Flores, F., Nielsen, M.T., Nafisi, M., Møldrup, M.E., Olsen, C.E., Motawia, M.S. and Halkier, B.A. (2009) Glucosinolate engineering identifies a γ -glutamyl peptidase. *Nat. Chem. Biol.* **5**, 575–577.
- Geu-Flores, F., Møldrup, M.E., Böttcher, C., Olsen, C.E., Scheel, D. and Halkier, B.A. (2011) Cytosolic γ -glutamyl peptidases process glutathione conjugates in the biosynthesis of glucosinolates and camalexin in *Arabidopsis*. *Plant Cell*, **23**, 2456–2469.
- Giavalisco, P., Hummel, J., Lisec, J., Inostroza, A.C., Catchpole, G. and Willmitzer, L. (2008) High-resolution direct infusion-based mass spectrometry in combination with whole ¹³C metabolome isotope labeling allows unambiguous assignment of chemical sum formulas. *Anal. Chem.* **80**, 9417–9425.
- Giavalisco, P., Li, Y., Matthes, A., Eckhardt, A., Hubberten, H.-M., Hesse, H., Segu, S., Hummel, J., Köhl, K. and Willmitzer, L. (2011) Elemental formula annotation of polar and lipophilic metabolites using ¹³C, ¹⁵N and ³⁴S isotope labelling, in combination with high-resolution mass spectrometry. *Plant J.* **68**, 364–376.
- Glazebrook, J. and Ausubel, F.M. (1994) Isolation of phytoalexin-deficient mutants of *Arabidopsis thaliana* and characterization of their interactions with bacterial pathogens. *Proc. Natl Acad. Sci. USA*, **91**, 8955–8959.
- Grzam, A., Martin, M.N., Hell, R. and Meyer, A.J. (2007) Γ -Glutamyl transpeptidase GGT4 initiates vacuolar degradation of glutathione S-conjugates in *Arabidopsis*. *FEBS Lett.* **581**, 3131–3138.
- Halkier, B.A. and Gershenzon, J. (2006) Biology and biochemistry of glucosinolates. *Annu. Rev. Plant Biol.* **57**, 303–333.
- Hegeman, A.D., Schulte, C.F., Cui, Q., Lewis, I.A., Huttlin, E.L., Eghbalnia, H., Harms, A.C., Ulrich, E.L., Markley, J.L. and Sussman, M.R. (2007) Stable isotope assisted assignment of elemental compositions for metabolomics. *Anal. Chem.* **79**, 6912–6921.
- Hell, R. and Wirtz, M. (2011) Molecular biology, biochemistry and cellular physiology of cysteine metabolism in *Arabidopsis thaliana*. *Arabidopsis Book*, **9**, e0154.
- Hertkorn, N., Frommberger, M., Witt, M., Koch, B.P., Schmitt-Kopplin, P. and Perdue, E.M. (2008) Natural organic matter and the event horizon of mass spectrometry. *Anal. Chem.* **80**, 8908–8919.
- Herzprung, P., Hertkorn, N., Friese, K. and Schmitt-Kopplin, P. (2010) Photochemical degradation of natural organic sulfur compounds (CHOS) from iron-rich mine pit lake pore waters – an initial understanding from evaluation of single-elemental formulae using ultra-high-resolution mass spectrometry. *Rapid Commun. Mass Spectrom.* **24**, 2909–2924.
- Hesse, H., Kreft, O., Maimann, S., Zeh, M. and Hoefgen, R. (2004) Current understanding of the regulation of methionine biosynthesis in plants. *J. Exp. Bot.* **55**, 1799–1808.
- Hirai, M.Y., Yano, M., Goodenowe, D.B., Kanaya, S., Kimura, T., Awazuhara, M., Arita, M., Fujiwara, T. and Saito, K. (2004) Integration of transcriptomics and metabolomics for understanding of global responses to nutritional stresses in *Arabidopsis thaliana*. *Proc. Natl Acad. Sci. USA*, **101**, 10205–10210.
- Hsieh, C.-L., Yeh, K.-W., de Kok, L.J., Pan, R.-N., Kuo, Y.-H. and Tseng, M.-H. (2012) Simultaneous determination of sulphur metabolites in *Arabidopsis*

- thazrliana via LC-ESI-MS/MS and ^{34}S -metabolic labelling. *Phytochem. Anal.* **23**, 324–331.
- Iijima, Y., Nakamura, Y., Ogata, Y. et al. (2008) Metabolite annotations based on the integration of mass spectral information. *Plant J.* **54**, 949–962.
- Janz, D., Behnke, K., Schnitzler, J.-P., Kanawati, B., Schmitt-Kopplin, P. and Polle, A. (2010) Pathway analysis of the transcriptome and metabolome of salt sensitive and tolerant poplar species reveals evolutionary adaptation of stress tolerance mechanisms. *BMC Plant Biol.* **10**, 150.
- Joosen, R.V., Arends, D., Li, Y., Willems, L.A., Keurentjes, J.J., Ligterink, W., Jansen, R.C. and Hilhorst, H.W. (2013) Identifying genotype-by-environment interactions in the metabolism of germinating Arabidopsis seeds using generalized genetical genomics. *Plant Physiol.* **162**, 553–566.
- Kanawati, B., von Saint Paul, V., Herrmann, C., Schäffner, A.R. and Schmitt-Kopplin, P. (2011) Mass spectrometric stereoisomeric differentiation between α - and β -ascorbic acid 2-O-glucosides. Experimental and density functional theory study. *Rapid Commun. Mass Spectrom.* **25**, 806–814.
- Kind, T. and Fiehn, O. (2006) Metabolomic database annotations via query of elemental compositions: mass accuracy is insufficient even at less than 1 ppm. *BMC Bioinformatics*, **7**, 234.
- Kind, T. and Fiehn, O. (2007) Seven golden rules for heuristic filtering of molecular formulas obtained by accurate mass spectrometry. *BMC Bioinformatics*, **8**, 105.
- Kopriva, S., Mugford, S.G., Matthewman, C. and Koprivova, A. (2009) Plant sulfate assimilation genes: redundancy versus specialization. *Plant Cell Rep.* **28**, 1769–1780.
- Krajewski, M.P., Kanawati, B., Fekete, A., Kowalski, N., Schmitt-Kopplin, P. and Grill, E. (2013) Analysis of Arabidopsis glutathione-transferases in yeast. *Phytochemistry*, **91**, 198–207.
- Krueve, A., Kaupmees, K., Liigand, J., Oss, M. and Leito, I. (2013) Sodium adduct formation efficiency in ESI source. *J. Mass Spectrom.* **48**, 695–702.
- Lee, B.-R., Huseby, S., Koprivova, A. et al. (2012) Effects of *fou8/fry1* mutation on sulfur metabolism: is decreased internal sulfate the trigger of sulfate starvation response? *PLoS One*, **7**, e39425.
- Li, X., Fekete, A., Englmann, M., Frommberger, M., Lv, S., Chen, G. and Schmitt-Kopplin, P. (2007) At-line coupling of UPLC to chip-electrospray-FTICR-MS. *Anal. Bioanal. Chem.* **389**, 1439–1446.
- Liao, S., Ewing, N.P., Boucher, B., Materne, O. and Brummel, C.L. (2012) High-throughput screening for glutathione conjugates using stable-isotope labeling and negative electrospray ionization precursor-ion mass spectrometry. *Rapid Commun. Mass Spectrom.* **26**, 659–669.
- Martin, M.N., Saladores, P.H., Lambert, E., Hudson, A.O. and Leustek, T. (2007) Localization of members of the γ -glutamyl transpeptidase family identifies sites of glutathione and glutathione S-conjugate hydrolysis. *Plant Physiol.* **114**, 1715–1732.
- Maruyama-Nakashita, A., Inoue, E., Watanabe-Takahashi, A., Yamaya, T. and Takahashi, H. (2003) Transcriptome profiling of sulfur-responsive genes in Arabidopsis reveals global effects of sulfur nutrition on multiple metabolic pathways. *Plant Physiol.* **132**, 597–605.
- Matsuda, F., Shinbo, Y., Oikawa, A., Hirai, M.Y., Fiehn, O., Kanaya, S., Saito, K. and El-Shemy, H.A. (2009) Assessment of metabolome annotation quality: a method for evaluating the false discovery rate of elemental composition searches. *PLoS One*, **4**, e7490.
- May, M.J. and Leaver, C.J. (1993) Oxidative stimulation of glutathione synthesis in Arabidopsis thaliana suspension cultures. *Plant Physiol.* **103**, 621–627.
- Mugford, S.G., Yoshimoto, N., Reichelt, M. et al. (2009) Disruption of adenosine-5'-phosphosulfate kinase in Arabidopsis reduces levels of sulfated secondary metabolites. *Plant Cell*, **21**, 910–927.
- Mugford, S.G., Lee, B.-R., Koprivova, A., Matthewman, C. and Kopriva, S. (2011) Control of sulfur partitioning between primary and secondary metabolism. *Plant J.* **65**, 96–105.
- Nakabayashi, R. and Saito, K. (2013) Metabolomics for unknown plant metabolites. *Anal. Bioanal. Chem.* **405**, 5005–5011.
- Nakabayashi, R., Sawada, Y., Yamada, Y., Suzuki, M., Hirai, M.Y., Sakurai, T. and Saito, K. (2013) Combination of liquid chromatography-Fourier transform ion cyclotron resonance-mass spectrometry with ^{13}C -labeling for chemical assignment of sulfur-containing metabolites in onion bulbs. *Anal. Chem.* **85**, 1310–1315.
- Nikiforova, V.J., Gakière, B., Kempa, S., Adamik, M., Willmitzer, L., Hesse, H. and Hoefgen, R. (2004) Towards dissecting nutrient metabolism in plants: a systems biology case study on sulphur metabolism. *J. Exp. Bot.* **55**, 1861–1870.
- Nikiforova, V.J., Kopka, J., Tolstikov, V., Fiehn, O., Hopkins, L., Hawkesford, M.J., Hesse, H. and Hoefgen, R. (2005) Systems rebalancing of metabolism in response to sulfur deprivation, as revealed by metabolome analysis of Arabidopsis plants. *Plant Physiol.* **138**, 304–318.
- Noctor, G., Queval, G., Mhamdi, A., Chaouch, S. and Foyer, C.H. (2011) Glutathione. *Arabidopsis Book*, **9**, e0142.
- Ohkama-Ohtsu, N., Radwan, S., Peterson, A., Zhao, P., Badr, A.F., Xiang, C. and Oliver, D.J. (2007a) Characterization of the extracellular γ -glutamyl transpeptidases, GGT1 and GGT2, in Arabidopsis. *Plant J.* **49**, 865–877.
- Ohkama-Ohtsu, N., Zhao, P., Xiang, C. and Oliver, D.J. (2007b) Glutathione conjugates in the vacuole are degraded by γ -glutamyl transpeptidase GGT3 in Arabidopsis. *Plant J.* **49**, 878–888.
- Ohkama-Ohtsu, N., Oikawa, A., Zhao, P., Xiang, C., Saito, K. and Oliver, D.J. (2008) A γ -glutamyl transpeptidase-independent pathway of glutathione catabolism to glutamate via 5-oxoprolin in Arabidopsis. *Plant Physiol.* **148**, 1603–1613.
- Ohkama-Ohtsu, N., Sasaki-Sekimoto, Y., Oikawa, A. et al. (2011) 12-oxo-phytodienoic acid-glutathione conjugate is transported into the vacuole in Arabidopsis. *Plant Cell Physiol.* **52**, 205–209.
- Ohta, D., Kanaya, S. and Suzuki, H. (2010) Application of Fourier-transform ion cyclotron resonance mass spectrometry to metabolic profiling and metabolite identification. *Curr. Opin. Biotechnol.* **21**, 35–44.
- Omranian, N., Mueller-Roeber, B. and Nikoloski, Z. (2012) PageRank-based identification of signaling crosstalk from transcriptomics data: the case of Arabidopsis thaliana. *Mol. BioSyst.* **8**, 1121–1127.
- Öztetik, E. (2008) A tale of plant glutathione S-transferases: since 1970. *Bot. Rev.* **74**, 419–437.
- Payne, T.G., Southam, A.D., Arvanitis, T.N. and Viant, M.R. (2009) A signal filtering method for improved quantification and noise discrimination in Fourier transform ion cyclotron resonance mass spectrometry-based metabolomics data. *J. Am. Soc. Mass Spectrom.* **20**, 1087–1095.
- Petersen, B.L., Chen, S., Hansen, C.H., Olsen, C.E. and Halkier, B.A. (2002) Composition and content of glucosinolates in developing Arabidopsis thaliana. *Planta*, **214**, 562–571.
- Ravilious, G.E. and Jez, J.M. (2012) Structural biology of plant sulfur metabolism: from assimilation to biosynthesis. *Nat. Prod. Rep.* **29**, 1138–1152.
- von Saint Paul, V., Zhang, W., Kanawati, B., Geist, B., Faus-Kessler, T., Schmitt-Kopplin, P. and Schäffner, A.R. (2011) The Arabidopsis glucosyltransferase UGT76B1 conjugates isoleucic acid and modulates plant defense and senescence. *Plant Cell*, **23**, 4124–4145.
- Saito, K. and Matsuda, F. (2010) Metabolomics for functional genomics, systems biology, and biotechnology. *Annu. Rev. Plant Biol.* **61**, 463–489.
- Sauter, M., Cornell, K.A., Beszteri, S. and Rzewuski, G. (2004) Functional analysis of methylthioribose kinase genes in plants. *Plant Physiol.* **136**, 4061–4071.
- Schmid, D.G., Grosche, P., Bandel, H. and Jung, G. (2000) FTICR-mass spectrometry for high-resolution analysis in combinatorial chemistry. *Bio-technol. Bioeng.* **71**, 149–161.
- Schütz, W., Hausmann, N., Krug, K., Hampp, R. and Macek, B. (2011) Extending SILAC to proteomics of plant cell lines. *Plant Cell*, **23**, 1701–1705.
- Shinbo, Y., Nakamura, Y., Altaf-Ul-Amin, M., Asahi, H., Kurokawa, K., Arita, M., Saito, K., Ohta, D., Shibata, D. and Kanaya, S. (2006) KNApSack: a comprehensive species-metabolite relationship database. *Biotechnol. Agric. For.* **57**, 165–181.
- Singh, R., White, M.A., Ramana, K.V., Petrash, J.M., Watowich, S.J., Bhatnagar, A. and Srivastava, S.K. (2006) Structure of a glutathione conjugate bound to the active site of aldose reductase. *Proteins*, **64**, 101–110.
- Smith, R. (2000) Evolution of ESI-mass spectrometry and Fourier transform ion cyclotron resonance for proteomics and other biological applications. *Int. J. Mass Spectrom.* **200**, 509–544.
- Sønderby, I.E., Geu-Flores, F. and Halkier, B.A. (2010) Biosynthesis of glucosinolates – gene discovery and beyond. *Trends Plant Sci.* **15**, 283–290.
- Sousa Silva, M., Gomes, R.A., Ferreira, A.E.N., Ponces Freire, A. and Cordeiro, C. (2013) The glyoxalase pathway: the first hundred years... and beyond. *Biochem. J.* **453**, 1–15.
- Stewart, B.J., Navid, A., Kulp, K.S., Knaack, J.L.S. and Bench, G. (2013) D-Lactate production as a function of glucose metabolism in *Saccharomyces cerevisiae*. *Yeast*, **30**, 81–91.

- Storozhenko, S., Belles-Boix, E., Babiychuk, E., Hérouart, D., Davey, M.W., Slooten, L., van Montagu, M., Inzé, D. and Kushnir, S.** (2002) γ -glutamyl transpeptidase in transgenic tobacco plants. Cellular localization, processing, and biochemical properties. *Plant Physiol.* **128**, 1109–1119.
- Tate, S.S. and Meister, A.** (1985) γ -Glutamyl transpeptidase from kidney. *Methods Enzymol.* **113**, 400–419.
- Tsuboi, S., Kobayashi, M., Nanba, M., Imaoka, S. and Ohmori, S.** (1990) S-(1,2-dicarboxyethyl)glutathione and activity for its synthesis in rat tissues. *J. Biochem.* **107**, 539–545.
- Tsuboi, S., Fujiwara, E., Ogata, K., Sakaue, A., Nakayama, T. and Ohmori, S.** (1993) Inhibitory effects of S-(1,2-dicarboxyethyl)glutathione on collagen-induced platelet aggregation; enhancements of cyclic AMP level and adenylate cyclase activity in platelets by S-(1,2-dicarboxyethyl)glutathione. *Biol. Pharm. Bull.* **16**, 1083–1086.
- Walker, S.H., Budhathoki-Uprety, J., Novak, B.M. and Muddiman, D.C.** (2011) Stable-isotope labeled hydrophobic hydrazide reagents for the relative quantification of N-linked glycans by electrospray ionization mass spectrometry. *Anal. Chem.* **83**, 6738–6745.
- Yoshimoto, N., Inoue, E., Saito, K., Yamaya, T. and Takahashi, H.** (2003) Phloem-localizing sulfate transporter, Sultr1;3, mediates re-distribution of sulfur from source to sink organs in Arabidopsis. *Plant Physiol.* **131**, 1511–1517.
- Zhao, F.J., Hawkesford, M.J. and McGrath, S.P.** (1999) Sulphur assimilation and effects on yield and quality of wheat. *J. Cereal Sci.* **30**, 1–17.